PLOS CLIMATE

RESEARCH ARTICLE

Climate warming erodes tropical reef habitat through frequency and intensity of episodic hypoxia

Noelle M. Lucey[1]*, **Curtis A. Deutsch**[2,3]*, **Marie-Hélène Carignan**[4], **Fanny Vermandele**[4], **Mary Collins**[1], **Maggie D. Johnson**[1,5], **Rachel Collin**[1], **Piero Calosi**[4]

1 Smithsonian Tropical Research Institute, Balboa Ancon, Panama, **2** School of Oceanography and Department of Biology, University of Washington, Seattle, Washington, United States of America, **3** Department of Geosciences and High Meadows Environmental Institute, Princeton University, Princeton, New Jersey, United States of America, **4** Marine Ecological and Evolutionary Physiology Laboratory, Département de Biologie, Chimie et Géographie, Université du Québec à Rimouski, Rimouski, Canada, **5** Red Sea Research Center, King Abdullah University of Science and Technology, Thuwal, Saudi Arabia

* luceynm@si.edu (NML); cdeutsch@princeton.edu (CAD)

Citation: Lucey NM, Deutsch CA, Carignan M-H, Vermandele F, Collins M, Johnson MD, et al. (2023) Climate warming erodes tropical reef habitat through frequency and intensity of episodic hypoxia. PLOS Clim 2(3): e0000095. https://doi.org/10.1371/journal.pclm.0000095

Editor: Cemal Turan, Iskenderun Technical University, TURKEY

Received: September 13, 2022

Accepted: January 18, 2023

Published: March 1, 2023

Peer Review History: PLOS recognizes the benefits of transparency in the peer review process; therefore, we enable the publication of all of the content of peer review and author responses alongside final, published articles. The editorial history of this article is available here: https://doi.org/10.1371/journal.pclm.0000095

Data Availability Statement: Data for this manuscript is available at: https://doi.org/10.6084/m9.figshare.14547519.v3.

Abstract

Climate warming threatens marine life by increasing metabolic oxygen demand while decreasing oxygen availability. Tropical species living in warm, low oxygen environments may be most at risk, but their tolerances and exposures to these stressors remain poorly documented. We evaluated habitat restrictions for two brittle star species from Caribbean coral reefs by integrating field observations, laboratory experiments and an ecophysiological model. The absence of one species from the warmest reefs results from vital activity restrictions during episodic low oxygen extremes, even though average conditions are well within physiological tolerance limits. Over the past decade, warmer temperatures have been significantly correlated with a greater frequency and intensity of hypoxic events. Continued warming will progressively exclude hypoxia-tolerant species, even if average oxygen remains constant. A warming-driven increase in frequency or intensity of low oxygen extremes could similarly accelerate habitat loss across other marine ecosystems.

Introduction

Tropical ecosystems are especially vulnerable to climate warming due to the prevalence of species living near their thermal optima, with low tolerance for temperatures outside the narrow range of tropical variability [1, 2]. The relationships between thermal tolerance, temperature variability, and the response to warming trends are well documented for terrestrial taxa, but their salience for marine species is unclear for two related reasons. First, rising ocean temperatures are linked to declining global oxygen content [3, 4], and while these stressors can act synergistically on physiological functions [5, 6], tropical species account for only 12.5% of those of which quantitative traits governing temperature-dependent oxygen tolerance have been measured [7]. Second, while temperature variability is low in both tropical marine and terrestrial

Funding: NL was supported by a fellowship awarded by Smithsonian Tropical Research Institute (STRI) and funding from M&J Bytnar. NL and RC were supported by a grant from the National Science Foundation (BIO-OCE 2048955) during manuscript preparation. A Smithsonian Institution Competitive Grant supported RC, and the Smithsonian Women's Committee award #53, STRI and the Smithsonian Marine Global Earth Observatory supported MDJ. The Natural Sciences and Engineering Research Council of Canada Discovery Program grant RGPIN-2015-06500 and RGPIN-2020-05627 and Canada Foundation for Innovation grant was awarded to PC, and supported PC, MHC and FV, as well as some of the research costs. The Quebec Center for Biodiversity Science Excellence Award supported MHC. FV was supported by the mobility grant from the University of Quebec in Rimouski foundation (FUQAR). The funders had no role in study design, data collection and analysis, decision to publish, or preparation of the manuscript.

Competing interests: The authors have declared that no competing interests exist.

environments, the relationship between oceanic oxygen and temperature variability from diel to decadal time scales are under sampled. A better understanding of both the tolerance for and exposure to increasing temperatures and declining oxygen in tropical oceans is therefore key to evaluating the vulnerability of the world's most productive and biodiverse ecosystems, including coral reefs, mangroves, and seagrass meadows.

As temperatures increase and oxygen levels decline, organisms' ability to fulfill their oxygen demand decreases [8], reducing energy available for critical ecological activity and long-term survival. The limits to metabolically viable habitat can be quantified by the Metabolic Index [9], a measure of the ratio of oxygen supply to demand that reflects both species physiological traits and environmental conditions. The Metabolic Index (Φ) has predicted species geographic range boundaries, and the loss of habitat from climate-induced changes in temperature and oxygen on seasonal, decadal, and geological timescales [8–11]. But the impact of short-term fluctuations in Φ on long-term environmental habitability is not known.

Oceanic conditions that are extreme, even if brief and/or infrequent, may also play an important role in mediating climate's impact on species fitness and habitability. Acute low oxygen events and ocean heatwaves both induce short-lived yet dramatic ecosystem changes [12–14]. But little is known about their co-occurrence [15] or their long-term consequences for species geography. This is because there is little sustained high-frequency data on the covariation of oxygen with temperature, or knowledge of the temperature-dependent hypoxia tolerances of resident species. Filling these data gaps is essential to establish mechanistic links between the extreme conditions of ocean 'weather' events and their long-term biological impacts.

Here we investigate how climate is restricting aerobic habitat in a major tropical reef. We do this by calibrating Φ with laboratory experiments on two reef–dwelling brittle star species and episodic temperature and oxygen extremes over a decadal time scale. The niche partitioning of the two species is only explained when the physiological and ecological components of the species' energetic demands are accounted for, and when temperature and oxygen effects are considered in combination. These combined effects explain current patterns of habitat exclusion and predict a rapidly increasing rate of tropical biodiversity erosion [16].

Results

Mapping a coral reef

We mapped the distribution of temperature, oxygen, and abundance of brittle stars in a large coral reef system on the Caribbean coast of Panama (Fig 1). Among the two species, not a single individual of *O. wendtii* was found close to the mainland, whereas *O. cinereum* dominated these inner bay sites. The relative abundance of *O. wendtii* increased on reefs closer to the outer bay, until there was an equal or higher abundance of *O. wendtii*.

The oxygen and temperature throughout the bay exhibit regional patterns resembling that of the brittle star abundance ratio, indicating a potential causal link. The lowest oxygen and highest temperatures co-occur near the mainland, at sites dominated by *O. cinereum* and where *O. wendtii* is excluded (Fig 1). Other environmental parameters (pH, salinity, chlorophyll) also varied throughout the bay, but variation was minimal relative to the changes in oxygen and temperature [17, 18].

A decade of weekly sampling at sites in the inner and outer bay confirm that these regional differences are persistent over time (Fig 1). The outer bay sites are consistently ~1˚C cooler than the inner bay throughout the year, while oxygen is generally higher except during June-July when differences disappear (S1 Fig, Table A in S1 Text). Temperature and oxygen are spatially and temporally negatively correlated, with the inner bay being slightly warmer, having

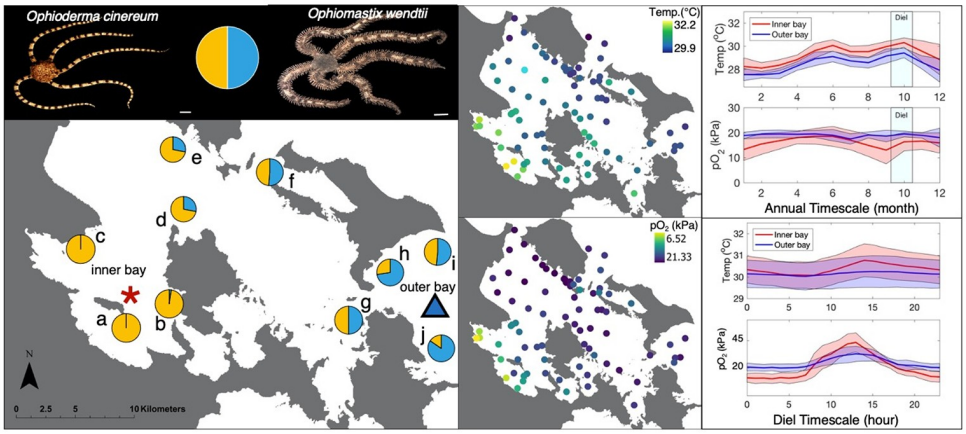

Fig 1. Distribution of brittle stars and oxythermal conditions over the past decade on the Caribbean coast of Panama. (*Left column*) Pie charts show proportion of individuals from two species of brittle star, *Ophioderma cinereum* (orange) and *Ophiomastix wendtii* (blue), found at each survey site. Animals were collected for laboratory experiments from 3 m at the inner bay (red asterisk) and outer bay (blue triangle) reef sites. (*Center column*) Daytime temperature (top) and pO_2 (bottom) surveyed on September 25th, 2017, at 3 m across 83 sites. (*Right column*) Time series of temperature and pO_2 over the mean seasonal cycle (upper panels) from a decade of weekly measurements 2010–2020 and the mean diurnal cycle (lower panels) from 37 d of hourly data collected between Oct.–Nov. 2019 (light blue shaded box). Solid colored lines in time series show average values and shading denotes the standard deviation. Base map from: https://stridata-si.opendata.arcgis.com/datasets/SI::bathymetry-of-the-republic-of-panama.

https://doi.org/10.1371/journal.pclm.0000095.g001

lower mean oxygen and greater oxygen variability, compared to the outer bay (Fig 1, top-right).

Hourly oxygen and temperature measured with sensors deployed directly within the reef matrix reveal the high-frequency variability associated with these spatial patterns (Fig 1). While diurnal temperature ranges are relatively small (~1˚) and similar across the bay, the daily oxygen fluctuations have a large amplitude, reaching a diurnal range of ~3x the mean value in the inner bay. The dynamic range of oxygen reflects the extremely high net primary productivity and rapid respiration at night, especially in the inner bay. The high productivity of the inner bay, coupled with lower abundance of the dominant brittle star predator [19] argues against food web dynamics being responsible for the exclusion of *O. wendtii* (Table B in S1 Text).

To evaluate whether these environmental gradients can mechanistically explain the difference in realized niches of these species, we determined their physiological tolerances to both elevated temperatures and low oxygen.

Physiological tolerances

We measured both species' physiological tolerance limits, resting and active metabolic rates, and survival after 4 h laboratory exposures to low oxygen, mimicking an *in situ* low oxygen episode (Fig 2, S1 Text).

Species sensitivity to low oxygen was measured as the critical oxygen pressure (P_{crit}) that can sustain resting aerobic metabolism [20, 21]. At ambient temperature (29˚C), both species had a comparable P_{crit}: 5.04 ± 1.72 kPa (mean ± SD); Fig 2A. At the highest temperatures recorded in the bay (32˚C) the P_{crit} of *O. cinereum* increased marginally (5.84 ± 2.14 kPa) but decreased in *O. wendtii* (2.77 ± 1.50 kPa). This lowered P_{crit} indicates *O. wendtii* is more tolerant to low oxygen–and therefore cannot account for its exclusion from the less oxygenated inner bay.

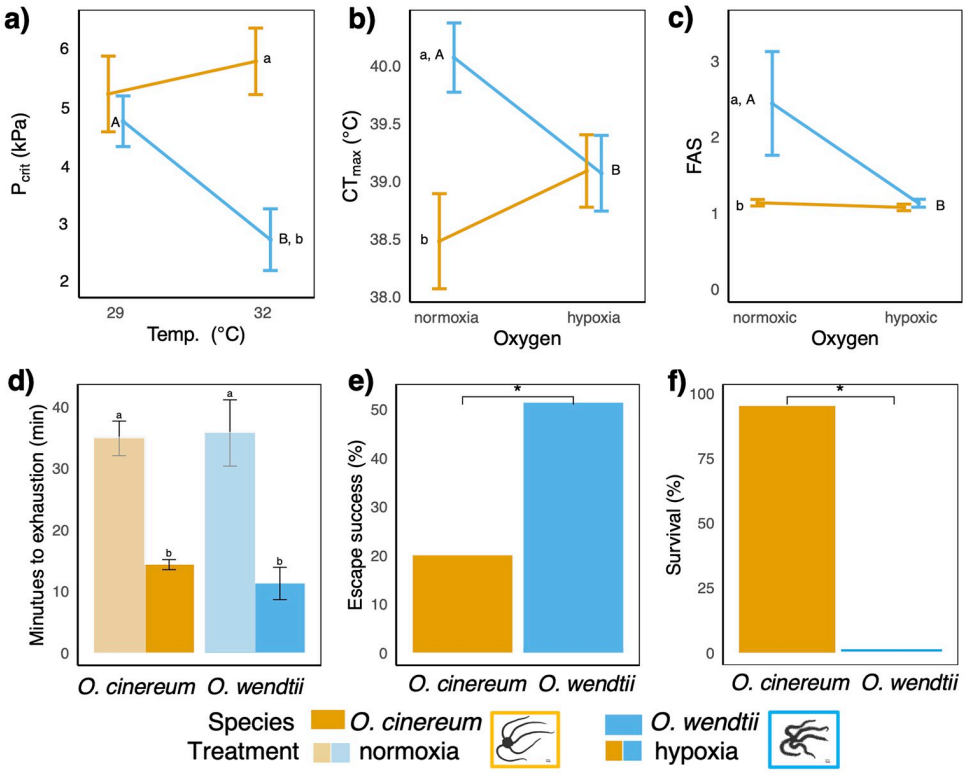

Fig 2. Physiological tolerances, behavior, and survival of *O. cinereum* (orange) and *O. wendtii* (blue). **(a)** Low pO_2 limits (P_{crit}) under ambient (29˚C) and high temperatures (32˚C). **(b)** Non-lethal upper thermal limits (CT_{max}) and **(c)** Factorial Aerobic Scope (FAS) under normoxia or low oxygen/hypoxia, 19.5 or 6.5 kPa, respectively. **(d)** Time to reach physical exhaustion in either normoxic conditions (light colors) or hypoxic conditions (dark colors) for each species. **(e)** Percentage of individuals that 'escaped' from experimental hypoxic conditions (< 6.5 kPa) by climbing out of a low oxygen layer. **(f)** Percentage of living individuals after experiencing low pO_2 (1.0 kPa) while resting, with all *O. wendtti* individuals dying after a 3.1 h duration. This time period is equivalent to one extreme low pO_2 event on the reef. Significantly different mean values ($p < 0.05$) in different treatments for the same species are indicated by capital letters, while significantly different mean values in the same treatment among different species are indicated by lowercase letters. Pairwise comparisons were conducted using the Estimated Marginal Means test with Least Significant Difference test correction. Error bars indicate ± SE.

https://doi.org/10.1371/journal.pclm.0000095.g002

As the inner bay is consistently warmer, the upper thermal limit of *O. wendtii* might explain its exclusion from the inner bay. To test this, we measured both species' Critical Thermal Maximum (CT_{max}), a widely used dynamic method to assess organisms' upper thermal limit (Fig 2B). Surprisingly, under normoxia, *O. wendtii* had a significantly higher upper thermal limit of 40.1 ± 1.1˚C compared to *O. cinereum* at 38.5 ± 1.6˚C ($p = 0.027$). Low oxygen, or hypoxia, significantly reduced the upper thermal limit of *O. wendtii* by 1.0˚C (to 39.1 ± 1.8˚C) and increased that of *O. cinereum* by 0.5˚C (to 39.1 ± 1.2˚C) (Fig 2B; $p = 0.024$, Table C in S1 Text). The two species' mean CT_{max} values were hence equivalent under low oxygen conditions.

The physiological tolerance traits measured in both species, coupled with the oxythermal gradient, eliminate some simple hypotheses for the observed distribution. First, while the inner bay is ~1.0˚C warmer than the outer bay, the CT_{max} of *O. wendtii* is ~1.5˚C higher than that of *O. cinereum*, indicating thermal tolerance alone cannot explain the different distributions. Second, resting critical oxygen tolerances (P_{crit}) are not substantially different between the species, at least at the ambient temperature of 29˚C. At the warmer temperatures of the inner bay *O. wendtii* has a higher tolerance for low oxygen relative to *O. cinereum*. Thus, low

oxygen tolerance under resting conditions also fails to explain the exclusion of *O. wendtii* in the inner bay, even after accounting for temperature dependence.

We determined the oxygen demand of each species under low oxygen and normoxic conditions, both at rest and after physical activity. The ratio of the maximum to minimum metabolic oxygen demand, termed Factorial Aerobic Scope (FAS) [22], was 2.5 times greater for *O. wendtii* than for *O. cinereum* under normoxic conditions: 2.44 ± 1.93 compared to 1.05 ± 0.26, as shown by a significant species effect (Fig 2C, $p = 0.002$, S2 Fig, Table C in S1 Text). The FAS of the two species did not differ under low oxygen, but the FAS of *O. wendtii* did decrease considerably under low oxygen compared to normoxia ($p = 0.027$). This decrease in the aerobic scope with strenuous activity under stressful conditions indicates that *O. wendtii* needs far more environmental oxygen to fully perform ecologically important activities such as reproduction, foraging and/or evading predation compared to *O. cinereum*. Additional assays, including behavioral escape trials and low oxygen survival rates, provide further support that *O. cinereum* is more hypoxia tolerant compared to *O. wendtii* (Fig 2E and 2F, S3 Fig).

Habitat exclusion

To evaluate the consequences of species' physiological traits on species distributions, we used the Metabolic Index (Φ), an ecophysiological framework based on the ratio of oxygen supply to metabolic demand at any environmental temperature and oxygen level. For environmental oxygen supply to sustain an organism's metabolic demand at rest, the Φ of an individual must be at least one ($\Phi \geq 1$) and, to enable maximum sustained activity, it must equal or exceed the factorial aerobic scope ($\Phi \geq$ FAS). The parameters of Φ correspond to two species traits—hypoxia tolerance and its temperature sensitivity (Eq 1)—and are calibrated from experimental P_{crit} data and its thermal variation (Fig 2).

For both species, the values of Φ vary strongly throughout the bay (Fig 3A and 3B), with lower values in the inner bay due primarily to the lower pO_2. The spatial gradient of Φ is amplified by temperature for *O. cinereum*, but weakened for *O. wendtii*, according to the temperature sensitivity of their P_{crit}. For both species, daytime Φ generally exceeded the value needed to support maximum metabolic activity across the bay.

To quantify how often the environmental conditions in the inner bay met both species' metabolic demands, we calculated Φ for *O. cinereum* and *O. wendtii* from diel and annual timescale data (Fig 3). During the 24 h diel period, Φ decreased nightly and increased daily for both species at both sites, primarily from lower pO_2, however, the magnitude of this diel cycle was greater in the inner bay (Fig 3C and 3E). In both sites, the average nightly Φ (Fig 3C and 3E, solid lines) was sufficient to meet both species oxygen demands, whether at rest or under peak activity (dashed black lines). However, the average daily cycle obscures the importance of episodic extremes of low Φ: extreme low pO_2 occurred approximately weekly in the inner bay and limited the aerobic scope of *O. wendtii* (i.e., Fig 3E—red shaded portion falling under dashed line; $\Phi <$ FAS), but not of *O. cinereum* (i.e., Fig 3C—all Φ values are above the dashed line that depicts *O. cinereum* FAS). Over the last ten years in the inner bay, daytime conditions also limited the aerobic scope of *O. wendtii*, providing further support that extreme Φ conditions render the inner bay unsuitable for *O. wendtii* (Fig 3F).

We determined how much time each species was exposed to environmental conditions that did not meet either their resting or active oxygen demands (i.e., conditions that limit activity). Hypoxia exposure times are identified when the Φ of each species falls below a threshold value of Φ_{crit}, where $\Phi_{crit} = 1$ in a resting state, and Φ_{crit} = FAS in an active state. *Hypoxia exposure* is then calculated as the total amount of time $\Phi < \Phi_{crit}$ within a measurement period. Hypoxia exposure was minimal for both species in the outer bay, regardless of energy state or time

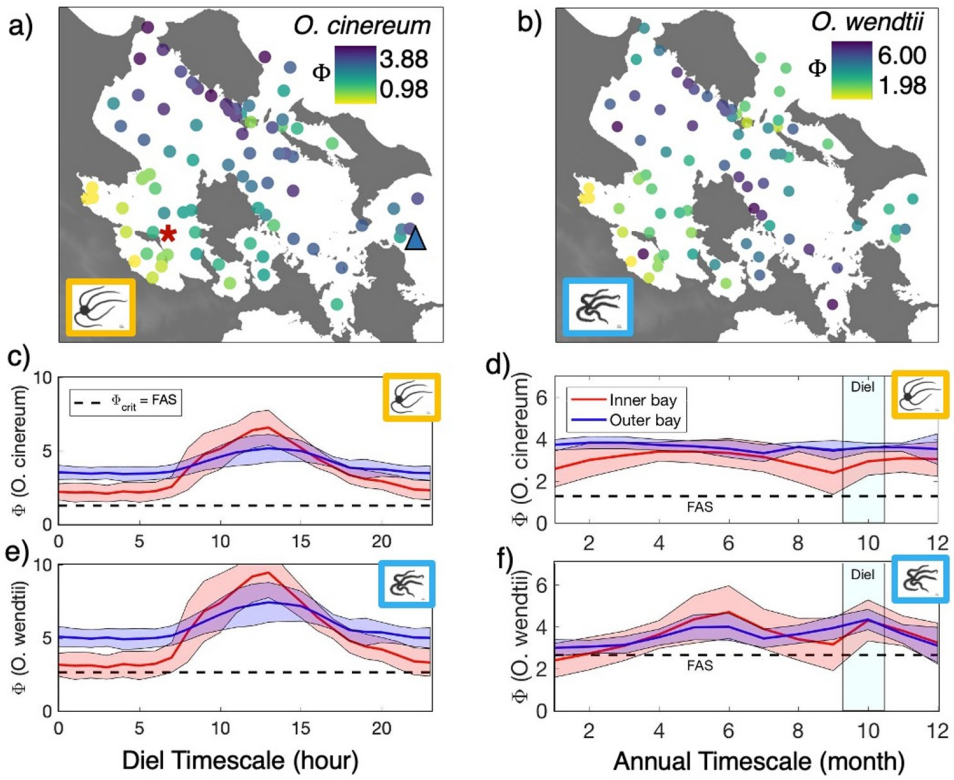

Fig 3. Distribution and time series of Φ throughout the reef for *O. cinereum* and *O. wendtii*. The Metabolic Index is computed from spatial and temporal observations of temperature and pO_2 (see Fig 1) and the temperature-dependent hypoxia traits for each species: *O. cinereum* **(c, d)**, *O. wendtii* **(e, f)**. The solid lines show average values and shading denotes the standard deviation around the mean. The Factorial Aerobic Scope (FAS) of each species (dashed lines) denotes the value of Φ below which maximum metabolic rate at the observed temperature would be limited by local oxygen availability. Base map from: https://stridata-si.opendata.arcgis.com/datasets/SI::bathymetry-of-the-republic-of-panama.

https://doi.org/10.1371/journal.pclm.0000095.g003

frame. At night, in the inner bay, hypoxia exposure was minimal for *O. cinereum* (0.03% during hourly 37-d diel timescale). However, hypoxia exposure of *O. wendtii* occurred 17% of the time during the same period (Fig 3C and 3E). Moreover, daytime hypoxia exposure during the last decade occurred ~0.02% of the time for *O. cinereum*, compared to 10% for *O. wendtii*. This suggests that infrequent episodic events of low Φ, reflecting fluctuating temperature-dependent oxygen, are not meeting the active metabolic requirements of *O. wendtii*, and that they account for the long-term exclusion of this species from the inner bay despite mean conditions being adequate to maintain maximum energetic demand.

Climate warming increases hypoxia exposure

We analyzed the relationship between temperature and pO_2 over the past decade to find out if hypoxia exposure increased with temperature. We find no significant relationship between temperature and pO_2. However, temperature is both positively and significantly correlated to pO_2 variance, such that the frequency and magnitude of both high and low pO_2 extremes increase with temperature, yielding a bivariate frequency distribution with a clear wedge-shaped pattern (Fig 4A). We then determined each the species' hypoxia exposure by mapping exclusion thresholds over the environmental 'wedge' using their respective Φ_{crit} values. The frequency of environmental conditions occurring under the species' exclusion thresholds

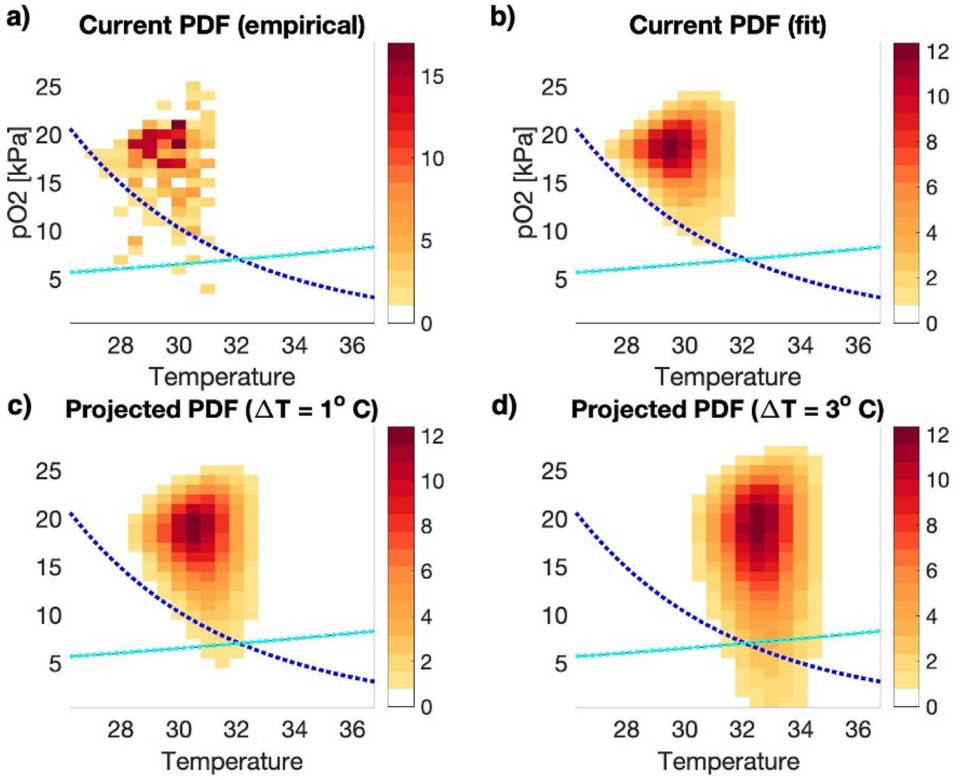

Fig 4. Bivariate frequency distribution of temperature and oxygen, from one decade of weekly daytime sampling. Orange coloration represents the environmental space of the inner bay, with panel **(a)** showing all measurements made from each temperature and oxygen combination during the 10-y sampling period. This is statistically modelled in panels **b-d** (Eq 2, S4 Fig). Light yellow colors indicate low occurrences or rare conditions and red colors indicate common, frequent (i.e., average) conditions. The ecophysiological exclusion thresholds ($\Phi = \Phi_{crit}$) are drawn over the environmental space for both *O. cinereum* (cyan lines) and *O. wendtii* (blue lines). Exposure to conditions that limit activity due to hypoxia are represented by the fraction of time that conditions fall below the species-specific thresholds ($\Phi < \Phi_{crit}$). **(c, d)** Projected future bivariate frequency distributions assuming temperatures increase by 1 or 3˚C, respectively. The frequency of stressful conditions (i.e., hypoxia exposure, $\Phi < \Phi_{crit}$) below the cyan and blue lines becomes more frequent as temperature rises.

https://doi.org/10.1371/journal.pclm.0000095.g004

determine how frequently they are exposed to metabolically limiting hypoxia (i.e., hypoxia exposure). The current hypoxia exposure of *O. wendtii* is ~8 times greater than *O. cinereum*, as shown by the higher frequency of conditions occurring under its exclusion threshold.

This observed temperature-pO_2 variance relationship is then used to project hypoxia exposure under scenarios of climate warming (Fig 4B, S4 Fig). If mean temperatures increase by 1˚C, the frequency and severity of pO_2 conditions also increase (Fig 4C). As warming approaches 3˚C, as projected for this region by Earth System Models by the end of this century, the frequency and severity of low pO_2 substantially increase [23] (Fig 4D). Such increases in hypoxia exposure will limit the activity of both brittle star species, as conditions will regularly fall below their respective exclusion thresholds ($\Phi < \Phi_{crit}$, Fig 4C and 4D, the increase of conditions occurring under both species exclusion thresholds). This future warming will increase the hypoxia exposure of *O. cinereum*, surpassing the exposure level that already excludes *O. wendtii*.

Hypoxia exposure on the reef can be evaluated across all combinations of active hypoxia tolerances and temperature sensitivities (i.e., species traits) based on the environmental conditions in the inner bay. Most known species trait combinations fall below the exclusion

threshold exhibited by *O. wendtii*, indicating that current conditions on this Caribbean reef are not metabolically habitable for most species sampled to date (Fig 5C; black points in yellow area). Yet there is a broad swath of viable trait space in this environment laying between that of *O. cinereum* and *O. wendtii*. Other tropical species may occupy this space, but their traits have not yet been measured. Even if this is the case, the frequency and intensity of low pO_2 would exclude all species within this range of physiological limits under a 3˚C warming scenario (Fig 5C; shifting exclusion thresholds from the black to red line).

Discussion

Our results have important implications for the role of climate in the maintenance and erosion of tropical marine biodiversity. First, the link between fine-scale spatial patterns of biogeography and aerobic habitat restrictions here supports similar conclusions based on large scale range limits across latitude and depth [7]. Second, the metabolic constraints on habitat occupancy become evident only when the role of temperature on oxygen variance is accounted for, and when both organismal physiological and ecological energetic demands are included. Neither temperature alone, nor the combined thermal and hypoxia tolerances in a resting state provide sufficient information to explain niche partitioning in the tropical marine organisms studied here. Third, survival in an aerobically demanding environment requires distinct adaptive strategies and energetic trade-offs among traits governing tolerance to temperature-dependent hypoxia. This is seen in the widely divergent active hypoxia tolerances and temperature sensitivities of both brittle star species found at the edges of habitable trait space for this reef (Fig 5). Given the high biological diversity currently making up tropical coral reefs, a greater sampling of these traits among reef biota is needed.

Finally, an increase in oxygen variability as temperatures rise will dramatically expedite reductions of available aerobic habitat. This is especially important in shallow tropical marine environments where Earth System Models and long-term observations indicate a relatively stable, or even increasing, O_2 as climate warms [24, 25]. Models that fail to reproduce sub-seasonal extremes and their response to climate change will greatly underestimate how quickly local extirpations are occurring in shallow environments, where oxygen variability rises sharply with warming. An expanded effort to measure temperature-dependent hypoxia tolerances of more tropical ectotherms, and to determine high-frequency covariation of environmental temperature and oxygen on other shallow ecosystems is required to evaluate how pervasive this mechanism is in accelerating the climate-driven loss of habitat and biodiversity.

Materials and methods

Species distributions

We used two ophuiroid species associated with tropical coral reefs: *Ophioderm cinereum* and *Ophiomastix wendtii* (Fig 1; MiAmbiante Permit SE/AP-20-18). To establish their relative abundance, we surveyed 10 coral reef sites throughout the bay between 3–5 m depth by collecting at least 30 individuals of either species. From this data, we determined the ratio of *O. cinereum* to *O. wendtii* at each site. We collected animals via SCUBA and snorkel by inspecting coral matrix for brittle star arms and then coaxing the animals out of the reef using a string and bait. Collection methodology was consistent across all sites to avoid potential bias.

Mapping a coral reef

Spatial analysis. We determined the spatial patterns of partial pressure of oxygen (pO_2) and temperature throughout the study area (i.e., Fig 1), by placing a YSI multiparameter sonde

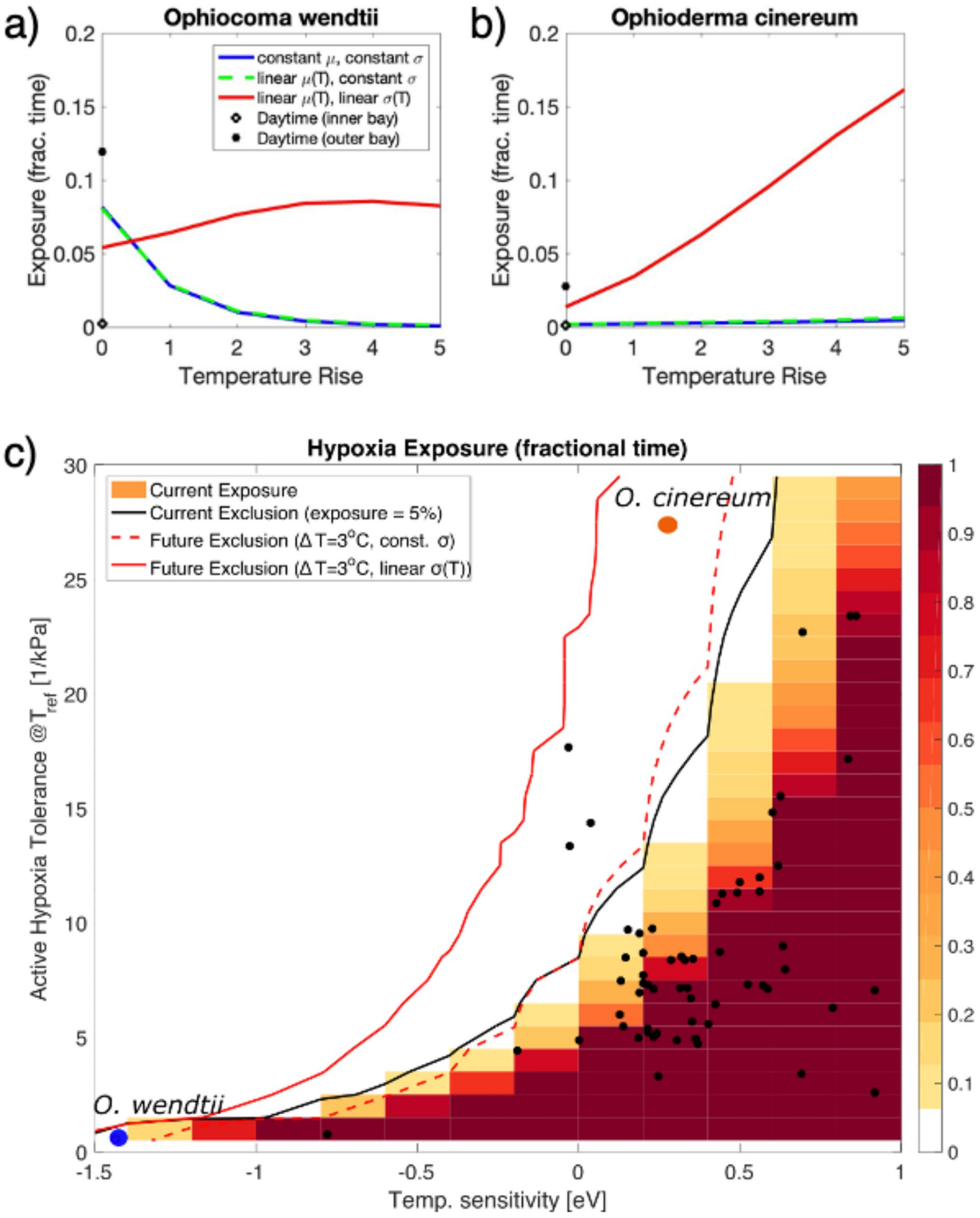

Fig 5. Impact of future warming on hypoxia exposure across species traits. (a, b) Exposure to hypoxia for both brittle star species, computed as a fraction of time with $\Phi <$ FAS in the current climate (dots) and under three different climate warming scenarios (curves). Observed relationship between temperature and pO_2 extrapolated to warmer conditions (Fig 4) yields a large increase in hypoxia exposure (red line), that disappears when increased pO_2 variance is neglected (green and blue lines). **(c)** Hypoxia exposure in the inner bay for a projected warming of 3˚C across the range of active hypoxia tolerance and temperature sensitivity traits (E_o and A_o) for known marine species globally (black dots) [7], and newly measured *O. cinereum* (orange circle) and *O. wendtii* (blue circle). Exposure on the reef would currently exclude most known species

at a 5% exclusion threshold (black line). If future pO_2 variance is constant, exclusion of additional trait space from exposure is minimal (dashed red curve), whereas the observed trend toward increased pO_2 variance erodes habitat for a broad swath of currently viable ecotypes (solid red curve), including *O. cinereum*.

https://doi.org/10.1371/journal.pclm.0000095.g005

(YSI EXO2 and EXO optical dissolved oxygen (DO) Smart Sensor–accuracy: 0.1 mg L^{-1}, Conductivity and Temperature Sensors–accuracy: 0.01˚C, Yellow Springs, USA) at 3 m in the water column at each of the 83 sites on 26 September 2017. Two boats were used to make all measurements between 08:00 and 17:30.

19-y hourly timeseries. We determined if temperature differed between the inner and outer bay sites by analyzing a 19 y, hourly continuous temperature record from loggers deployed directly on a concrete block nestled within the reef matrix at a depth of 3 m (Hobo Onset loggers; Dec. 2000 –May 2019; datasets provided by the STRI Physical Monitoring Program; S1 Fig).

37-day hourly timeseries. To monitor the joint variation in temperature and pO_2 through time at both the inner and outer bay sites, we deployed temperature, DO, and conductivity loggers at a depth of 3 m directly within the coral reef matrix (U26-001 HOBO DO Logger–accuracy: 0.2 mg L^{-1}; U24-002 Conductivity Logger; Onset, MA). Loggers were 10 cm from living coral and reef structure (i.e., logger was at the same height at the coral, with coral surrounding the logger). They were deployed between October and November 2019 and took measurements hourly. pO_2 measurements were calculated from DO, conductivity and temperature. Measurement precision was based on comparisons to measurements made in the field before and after calibration checks with a YSI Pro2013 multi-parameter handheld (accuracy: DO 0.2 mg L^{-1}, temperature 0.35 ˚C, conductivity 0.5%).

10-y weekly timeseries. Weekly data was collected during the day from Jan 2010 to March 2020 with a handheld YSI multiparameter sonde which was lowered to a depth of 10 meters in the water column above the benthos (YSI EXO2 and EXO optical DO–accuracy 0.1 mg L^{-1}; Conductivity and Temperature Sensors–accuracy 0.01˚C, Yellow Springs, United States; STRI Physical Monitoring Program). Sensors were calibrated monthly following the manufacturers' instructions. The weekly monitoring sites are approximately 10 m from the benthos and provide comprehensive overview of the oxygen conditions occurring in the area, as well as represent conservative estimates for the oxygen fluctuations occurring on the reef (datasets provided by MarineGEO and the STRI Physical Monitoring Program).

GPS coordinates for physical data collection sites and species abundance collection sites are provided in the raw datasets (S1 Text). A distance of ~ 10 km separates the outer bay reef site (37-d hourly record) from the outer bay weekly monitoring site (10-y weekly record, 'Colon'), however discreet measurement calibrations between these outer bay sites validated outer bay site pairing.

Experimental details

For all experiments, we hand collected *O. cinereum* from both the inner and outer bay sites, and *O. wendtii* from the outer bay sites (Fig 1). Within 2–4 h of collection, they were transported back to the Bocas Research Station (BRS) in temperature-stable coolers and were immediately transferred to 40 L tanks and maintained with flowing seawater at ambient temperature until the start of the experiments (within ~10 d of collection). Prior to the experiments, individuals were fed small pieces of fish in the laboratory; they were starved for 48 h before the SMR trials and not fed anything thereafter.

To maintain/establish oxygen treatments before for the SMR, MMR, CT_{max} trials, individuals were moved to 4 L aquarium tanks that were either bubbled with pure nitrogen to reduce

oxygen levels (i.e., hypoxic treatment; pO_2, 6.5 kPa; DO, 2 mg L^{-1}), or bubbled with air to maintain normoxic conditions, pO_2, 19.5 kPa; DO, 6 mg L^{-1}. pH was not experimentally modified and did not decrease during these experiments. Treatment acclimation lasted for 4 h prior to trials. During this time aquaria were kept in water baths with aquarium heaters to ensure temperature remained constant at 29˚C and salinity at 34 ppt. Filtered (0.45 μm) seawater was used for all trials.

Physiological tolerances

P_{crit} experiments were conducted on 42 *O. cinereum* and 23 *O. wendtii* individuals. Individuals were gently rinsed with well-oxygenated filtered seawater and put into closed respirometry chambers. Equal numbers of trials were performed at 29 and 32˚C. For trials at 32˚C, the seawater was ramped from ambient 29 to 32˚C in 1 h in an isolated tank before being placed in the respiratory chamber. The initial pO_2 value was 19.5 ± 0.29 kPa for all trials. pO_2 in the chamber was recorded with fiber-optic sensor technology (Fibox 4 and Pst-3 sensors, PreSens, Regensburg, Germany), every minute until the concentration fell to 1.0 kPa (0.3 mg L^{-1}). Temperature in the water bath was recorded simultaneously with the Fibox 4, as well as a thermocouple thermometer (HH802U, OMEGA, Canada—accuracy 0.1˚C). Upon reaching the oxygen depletion target in the chamber, each individual was promptly moved into ambient, oxygenated water. No individuals died immediately after P_{crit} trials. Wet weight was measured using a precision balance (PL6001E, Mettler Toledo–accuracy 0.1 g) and volume was measured via displacement using a graduated cylinder and beaker. After taking morphometric measurements individuals were then moved to well-oxygenated recovery tanks with flowing, ambient temperature seawater for 24 h. Survival was documented after the 24 h recovery period, i.e., Fig 2F. We determined the P_{crit} for each individual using broken stick regression which fits two regression lines through the data using the respR package [26]. The intersection of the two regression lines is the critical point and defines P_{crit}.

Acute upper thermal limits (CT_{max}) were measured in *O. cinereum* (32 indiv.) and *O. wendtii* (16 indiv.) under hypoxic (6.5 kPa, 2 mg L^{-1}) and normoxic (19.5 kPa, 6 mg L^{-1}) conditions, using the onset of spasm as the endpoint (defined below in more detail). Trials were conducted following exposure to two oxygen treatments representative of a single nightly drop in oxygen (4 h hypoxia; 6.5 kPa, temp. 29˚C, salinity 34, 2.0 mg L^{-1}) or normoxic conditions on the reef (4 h normoxia; >19.5 kPa, temp. 29˚C, salinity 34, 6.0 mg L^{-1}). They were then transferred in 300 mL glass bowls containing water kept at their corresponding pO_2 treatment and left to rest for 10 min at 29˚C. Water temperature was then increased at a rate of 1˚C min^{-1} using a thermostatic water bath (Cole-Parmer ® StableTemp® Digital General-Purpose Baths, Cole-Parmer Canada, Canada) and individuals were observed continuously until they reached the endpoint (see S1 Text for video A link to CT_{max} trial). The corresponding temperature was identified as their CT_{max} temperature and measured using a thermocouple thermometer (HH802U, OMEGA) [27, 28]. Given the scarce literature available for CT_{max} measurements on echinoderms, initial trials were performed to identify a repeatable behavioral response, assayable for both species, that would correspond to the equivalent of onset of spasm for brittle stars. From these preliminary trials, we define CT_{max} as the non-lethal temperature at which animals rapidly curl their arms together and become stiff and completely unresponsive to touch. Immediately after reaching the endpoint, individuals were removed, and their wet weights were measured before transferring to an ambient temperature recovery tank. Animal mass was used as a covariate in the statistical models to rule out any statistical differences in size. Survival was assessed after 24 h and only surviving individuals were included in CT_{max}

dataset. Note that CT_{max} and P_{crit} measurements are strictly designed to define and compare the relative physiological performances, behavioral responses, and tolerance levels for species' comparison (S1 Text).

Oxygen demand

Prior to the upper thermal limit measurements (CT_{max}), oxygen consumption rates (MO_2) at rest (i.e., standard metabolic rate; SMR) and after/at exhaustion (i.e., maximum metabolic rate; MMR) were measured in *O. cinereum* (32 indiv.) and *O. wendtii* (16 indiv.), under either hypoxic or normoxic conditions. We assayed metabolic rates using closed cell respirometry. Oxygen partial pressure (in μmols) inside the respirometry chambers were measured every 15 min using fiber-optic sensor technology (Fibox 4 and Pst-3 sensors, PreSens, Regensburg, Germany), for two hours or until the oxygen levels in the chambers were reduced to 80% of the initial saturation level. Sensors were individually calibrated just before the experiment, using two-points (0–100% air saturation) with the manufacturer's method at ambient temperature (29˚C). Each chamber was sealed and included a mesh screen that divided a magnetic stir bar from the main chamber area. Chambers were placed over a multi-channel magnetic stirrer (Mix 15 Eco Stir) to ensure gentle mixing throughout the trial and prevent oxyclines from forming inside the chambers.

Standard metabolic rates (SMR) were measured under resting conditions. We acclimated an animal to the selected treatment for 3 h before placing them into their respirometry chamber for an additional acclimation period of 1 h while continuing their hypoxic or normoxic treatment. After the SMR trial, animals were then returned to separate maintenance tanks for 2 d before undergoing MMR measurements.

Individual MMR was measured following a post-exercise methodology that was adapted for the ophiuroids [29, 30]. Trials started with 4 h treatment acclimations, individuals were moved to a new tank with filtered seawater (47 mm GF/F glass microfiber filter, Whatman®, Buckinghamshire, United Kingdom) matching their oxygen treatment. Each individual's maximum metabolic rate (MMR) was then measured by exhausting the individual by manually flipping the animal onto its back and repeating when it righted, until they remained upside-down without any attempt to right themselves for more than 1 min (i.e., exhaustion, Video B in S1 Text shows the exhaustion method). The time it took each individual to reach exhaustion was recorded. At this point of exhaustion, we moved individuals into respirometry chambers and immediately began measuring oxygen consumption (MO_2) as in SMR trials above, obtaining the MMR.

To minimize microbial respiration, all respirometry chambers were transferred and closed in a clean tank filled with filtered seawater (Whatman ®). We monitored microbial respiration by including two chambers filled only with water from the clean tank, for each trial, or blanks, where six individuals were undergoing measurements. Oxygen consumption rates (in $\mu mol\ h^{-1}\ mg^{-1}$) were individually calculated from blank corrected animals' fluxes ($\mu mol\ L^{-1}\ h^{-1}$) standardized by their wet mass (mg). Microbial respiration was effectively contained to marginal fluxes and the animals' oxygen consumption was constant (i.e., linear decrease in oxygen concentration during trials). We corrected the chambers' volumes by subtracting the stirrer's and the individuals' volumes from their total capacity.

The aerobic scope–both absolute (AAS) and factorial (FAS) of each individual was calculated in absolute terms: MMR–SMR and factorial terms: SMR: MMR [29]. FAS values < 1 were replaced by 1 as aerobic scope must be a positive number, after determining no statistical changes between unmodified vs. modified FAS. After the MMR trial, individuals were rested in a maintenance tank overnight, and CT_{max} tested the following day (see above).

Escape behavior

To determine if *O. cinereum* and *O. wendtii* exhibited hypoxia escape behaviors, we simulated hypoxia shoaling in an oxygen-gradient chamber. The chambers consisted of a clear plexiglass 50 cm tall column (S3 Fig). Freshwater was mixed with seawater to slightly reduce the salinity in the top normoxic water layer, while deoxygenated seawater was pumped in from below to create the bottom hypoxic layer. The salinity differed by 2–3 ppt between water layers. We tested a total of 55 individuals, 35 *O. cinereum* and 20 *O. wendtii*. Individuals were placed in an oxygen-gradient chamber and allowed to rest for 1 h before the trial with an escape ladder inserted into the chamber so that it was reachable to the individual. This allowed individuals to explore the chamber, discover the ladder and acclimate to the new surroundings and salinity. After the resting period, deoxygenated seawater was slowly added to the bottom of the chamber to avoid mixing with the top layer, until the bottom half of the chamber was filled with hypoxic water (1.13 ± 0.41 mg L^{-1}), while the top half of chamber remained normoxic (6.34 ± 0.23 mg L^{-1}). This was equivalent to pO_2 of ~3.7 kPa in the hypoxic layer and 20.0 kPa in the normoxic later. Trials began as soon as hypoxic water was introduced and lasted 1 h or until the individual climbed to the surface. We recorded the success of each individual to 'escape' from hypoxic conditions by climbing up the ladder into the normoxic area. The time to escape (min), as well as any effort made to escape was also recorded.

No individuals died during respiration or behavior trials.

Habitat exclusion by episodic hypoxia waves

The metabolic index (Φ) is calculated using the following equation:

$$\Phi = AB^{\varepsilon} pO_2 \ exp\left\{\frac{E}{k_B}\left[\frac{1}{T} - \frac{1}{T_{ref}}\right]\right\} \quad (1)$$

where A_O is the ratio of rate coefficients for O_2 supply capacity relative to resting metabolic rate at a reference temperature (T_{ref} = 15˚C), B^{ε} is the body mass scaling, pO_2 in ambient O_2 pressure, E_O is the temperature dependence of the O_2 supply/demand ratio, k_B is the Boltzmann's constant, and T is temperature [9]. The physiological parameters of Φ are obtained from fitting a regression to the natural log of the measured P_{crit} values of each species at the reference temperature. The slope and intercept are set to E_O and A_O, respectively. In this study, we calculated Φ for both species, through time, from temperature and pO_2 taken from the 37-d hourly timeseries (diel timescales) as well as the 10-y weekly timeseries (annual timescales), at both sites (physical parameters = pO_2 and temperature).

Climate warming increases hypoxia exposure

To project the frequency of hypoxic extremes as the reef warms, we modeled the bivariate frequency distributions of local temperature and pO_2. The probability of a given combination of environmental temperature (T) and pO_2 was modeled as a product of separate probability distributions functions (pdf's) for temperature (n) and pO_2 (m):

$$f(\mathrm{T}, \mathrm{pO_2}) = \mathrm{n(T)}^{*}\mathrm{m}(\mathrm{T}, pO_2)$$

The pdf for temperature is modelled as normally distributed, with statistics (mean, standard deviations) that are assumed independent of pO_2. In contrast, based on the long 'tail' of low pO_2, its pdf is modeled as a lognormal distribution. We use a log-transformed version of pO_2, $\hat{p} = \log(1.01 - pO_2/0.3)$, where the normalization (0.3 atm) is chosen to be above the maximum observed pO_2, so that $\hat{p}$ varies from 0–1 and is approximately normally distributed.

Based on the wedge-shaped bivariate histogram of T and pO_2 (Fig 4A), the statistics of pO_2 are allowed to change linearly with T. Under these conditions, we can write the joint probability of observing an environment with a given combination of T and pO_2 as:

$$f(T, pO_2) = a_1 \exp\left(\frac{T - \mu_T}{\sigma_T}\right)^2 \exp\left(\frac{\hat{p} - \mu_{\hat{p}}(T)}{\sigma_{\hat{p}}(T)}\right)^2 \quad (2)$$

The mean and variance of $\hat{p}$ are assumed to be linear functions of T, so that $\mu_{\hat{p}}(T) = b_1 + b_2 T$ and $\sigma_{\hat{p}}(T) = c_1 + c_2 T$.

The joint pdf (i.e., *f*) thus has 7 parameters: α_1, μ_T, σ_T, b_1, c_1, b_2, c_2, which we determined by finding the best fit to the binned 2D histogram of T and pO_2. We chose measurements in the inner bay in the 10-y weekly daytime record (Fig 4B), because this decadal timescale includes the relationships between variation of T and pO_2 most relevant to climate change. The fits are highly significant ($p < 1\ e^{-30}$, $R_2 = 0.56$, d.f. = 118), including for the slope of pO_2 variance versus temperature, $c_2 = 0.078913$ (s.e. = 0.019927, $p = 1\ e^{-4}$).

Experimental statistical analyses

We determined if SMR, MMR, and FAS measured in normoxic conditions were different from those measured under hypoxia using a 2-way ANCOVA with 'treatment', 'species,' and their interaction as factors, and wet weight as the covariate. Similarly, we determined the relative importance of species and either oxygen treatment or temperature treatment for CT_{max} and P_{crit} using a 2-way ANOVA, again with wet weight as a covariate. Individuals used in MMR trials prior to CT_{max} trials made up 21% of the total number used in CT_{max} trials. We tested whether this prior history impacted CT_{max} results by adding 'history' to the model as a covariate. No differences were found, so 'history' was removed from the model. Data was assessed for normality by building histograms of the residuals, and checked for non-linearity, unequal error variances, and outliers by plotting the residuals against fitted values. Weight was removed if it was not significant. Metabolic rate and P_{crit} data were log transformed to address over-dispersion and meet assumptions of normality.

To test the effect of species on hypoxia escape success, we initially constructed a binomial Generalized Linear Model with 'species' as the fixed factor using the logit link (GLMs, R package nlme v. 3.1–131). The oxygen measured during each trial in the hypoxic layer was added as a covariate, however 'oxygen' did not exert a significant effect and was removed from the final model [31]. Normality was again assessed by building histograms of the residuals, and residuals plotted against fitted values were used to detect non-linearity, unequal error variances, and outliers. Data was balanced and not over-dispersed, and the oxygen level covariate removed [32–34].

It is possible that the traits of *O. cinereum* individuals from the inner bay are influenced by local adaptation. We tested this at a cursory level by collecting equal numbers of *O. cinereum* individuals from both sites for all experiments (SMR, MMR, P_{crit}, CT_{max} trials, exhaustion time, behavior, and survival). We determined whether there was a statistical difference between those collected from the inner bay compared to outer bay populations, by comparing traits as a function of site and treatment (i.e., ANCOVA and ANOVA, as in Tables C, D in S1 Text, respectively), with the assumption that a statistical difference would indicate either adaptations or plasticity differences. We found no statistical differences in any traits from *O. cinereum* individuals originating from the inner bay compared to the outer bay sites, and therefore use data from *O. cinereum* individuals collected from all sites in the comparisons between species (Tables C, D in S1 Text).

Statistical analyses were performed by using the statistical software R v.3.1.3 [33] and Matlab. A detailed summary of the responses in each experiment can be found in S1 Text.

Supporting information

S1 Fig. Seawater temperature timeseries values over a 20 y time frame. Measurements were collected every hour with probes deployed on the seafloor (3 m) in the reef matrix at locations near both sites. A 2 y rolling average is displayed, fitted with linear trend lines for each site (data provided by the STRI Physical Monitoring Program).
(PNG)

S2 Fig. The metabolic responses of *O. cinereum* (orange lines) and *O. wendtii* (blue lines) presented as reaction norm plots. Resting metabolic rates (SMR) **(a)**, maximum metabolic rates (MMR) **(b)**, and (unmodified) factorial aerobic scope (FAS) **(c)**, under normoxia or hypoxia, 19.5 or 6.5 kPa (6 or 2 mg L^{-1}), respectively. Significantly different mean values ($p < 0.05$) in different treatments for the same species are indicated by capital letters, while significantly different mean values in the same treatment among different species are indicated by lowercase letters. Pairwise comparisons were conducted using the Estimated Marginal Means test with Least Significant Difference test correction. Error bars indicate ± SE. At rest, both species showed comparable oxygen demand in both oxygen treatments **(a)**. However, the two species' oxygen demands significantly differed after physical activity **(b)**. The MMR of *O. wendtii* was 1.75 times higher than *O. cinereum* ($p < 0.005$), and the FAS was 2.5 times greater than *O. cinereum* under normoxic conditions. The FAS of the two species did not differ under hypoxia, but the FAS of *O. wendtii* did decrease considerably under hypoxia compared to normoxia ($p = 0.027$).
(TIFF)

S3 Fig. Conceptual diagram of O_2-gradient chamber. The left image shows a resting brittle star at the bottom of the chamber in normoxic water; the middle image shows hypoxic water entering through the bottom of the chamber and moving up in the water column to the midpoint (25 cm), and the right image shows the point at which the brittle star is high enough in the chamber to be considered an escapee. In coastal areas where rapid shoaling of hypoxic waters is common, the ability of mobile individuals to quickly sense deleterious conditions and relocate to more oxygenated surface waters can mean the difference between life and death. We mimicked hypoxia stratification in the laboratory to test the ability of each species to sense and climb out of a hypoxic water layer. *Ophioderma cinereum* individuals were 2.5 times more likely to escape from hypoxic water than *O. wendtii* (51.4% versus 20% respectively; $p = 0.026$). Of those that did crawl out of the hypoxic layer, they did so in 15 min on average and this did not differ between species. *Ophioderma cinereum* appears to be much more capable of utilizing its energetic 'window' to relocate to better environmental conditions when conditions threaten their metabolic capacity. This further strengthens the hypothesis that oxygen limitation from necessary activities sets these two species apart.
(PNG)

S4 Fig. a) Bivariate frequency distribution of temperature and partial pressure of oxygen (pO2) in the inner bay, based on 10-y weekly daytime measurements. b) Modeled distribution assuming the statistics (mean μ, standard deviation σ) of temperature (T) are independent of pO2, whereas the statistics of pO2 are allowed to change linearly with T, leading to the best fit (b). If pO2 variance is ignored (i.e., constant σ, panel c), or if only a mean change in temperature occurs with no variance (d), exposure to hypoxia increases, but only due to species'

biological sensitivities (Eo > 0). Reference line (black) is Pcrit * FAS for O. cinereum, and forms this species' temperature dependent exclusion threshold.
(TIFF)

S1 Text.
(DOCX)

Acknowledgments

We thank STRI Bocas Research Station staff, STRI Monitoring Program, MarineGeo (#78), as well as K Birkenmayer, L Beckman, and A Herwig for experimental assistance. We also thank Y Kai and Madeleine-Zoé Corbeil-Robitaille for providing graphical artwork, and the Panamanian government for permission to conduct this research in Bocas del Toro, Panama.

Author Contributions

Conceptualization: Noelle M. Lucey, Curtis A. Deutsch, Marie-Hélène Carignan, Fanny Vermandele, Mary Collins, Piero Calosi.

Data curation: Noelle M. Lucey, Curtis A. Deutsch.

Formal analysis: Noelle M. Lucey, Curtis A. Deutsch.

Funding acquisition: Noelle M. Lucey, Maggie D. Johnson, Rachel Collin.

Investigation: Noelle M. Lucey, Curtis A. Deutsch, Marie-Hélène Carignan, Fanny Vermandele, Mary Collins, Piero Calosi.

Methodology: Noelle M. Lucey, Curtis A. Deutsch, Marie-Hélène Carignan, Fanny Vermandele, Mary Collins, Piero Calosi.

Project administration: Noelle M. Lucey, Rachel Collin.

Resources: Noelle M. Lucey, Curtis A. Deutsch, Maggie D. Johnson, Rachel Collin, Piero Calosi.

Supervision: Rachel Collin, Piero Calosi.

Validation: Noelle M. Lucey.

Visualization: Noelle M. Lucey, Curtis A. Deutsch, Piero Calosi.

Writing – original draft: Noelle M. Lucey.

Writing – review & editing: Noelle M. Lucey, Curtis A. Deutsch, Marie-Hélène Carignan, Fanny Vermandele, Mary Collins, Maggie D. Johnson, Rachel Collin, Piero Calosi.

References

1. Tewksbury JJ, Huey RB, Deutsch CA. Putting the heat on tropical animals. Science. 2008; 320(June 6):1296–7.
2. Rummer JL, Couturier CS, Stecyk JAW, Gardiner NM, Kinch JP, Nilsson GE, et al. Life on the edge: Thermal optima for aerobic scope of equatorial reef fishes are close to current day temperatures. Global Change Biology. 2014; 20(4):1055–66. https://doi.org/10.1111/gcb.12455 PMID: 24281840
3. Schmidtko S, Stramma L, Visbeck M. Decline in global oceanic oxygen content during the past five decades. Nature. 2017; 542:335–51. https://doi.org/10.1038/nature21399 PMID: 28202958
4. Ito T, Minobe S, Long MC, Deutsch C. Upper ocean O2 trends: 1958–2015. Geophysical Research Letters. 2017; 44(9):4214–23.
5. Fry F. Effects of the environment on animal activity. Toronto: University of Toronto Press; 1947. 1–62 p.

6. Pörtner HO. Oxygen- and capacity-limitation of thermal tolerance: a matrix for integrating climate-related stressor effects in marine ecosystems. Journal of Experimental Biology. 2010; 213(6):881–93. https://doi.org/10.1242/jeb.037523 PMID: 20190113

7. Deutsch C, Penn JL, Seibel B. Metabolic trait diversity shapes marine biogeography. Nature. 2020 Sep; 585(7826):557–62. https://doi.org/10.1038/s41586-020-2721-y PMID: 32939093

8. Howard EM, Penn JL, Frenzel H, Seibel BA, Bianchi D, Renault L, et al. Climate-driven aerobic habitat loss in the California Current System. Science Advances. 2020;(May):1–11. https://doi.org/10.1126/sciadv.aay3188 PMID: 32440538

9. Deutsch C, Ferrel A, Seibel B, Pörtner HO, Raymond BH. Climate change tightens a metabolic constraint on marine habitats. Science. 2015; 348(6239):1132–6.

10. Penn J, Deutsch C, Payne J, Sperling E. Temperature-dependent hypoxia explains biogeography and severity of end-Permian marine mass extinction. Science. 2018; https://doi.org/10.1126/science.aat1327 PMID: 30523082

11. Duncan MI, James NC, Potts WM, Bates AE. Different drivers, common mechanism; the distribution of a reef fish is restricted by local-scale oxygen and temperature. Conservation Physiology. 2020; (October).

12. Chan F, Barth JA, Lubchenco J, Kirincich A, Weeks H, Peterson WT, et al. Emergence of anoxia in the California current large marine ecosystem. Science. 2008; 319(5865):920. https://doi.org/10.1126/science.1149016 PMID: 18276882

13. Frölicher TL, Laufkötter C. Emerging risks from marine heat waves. Nature Communications. 2018;2015–8.

14. Johnston MA, Nuttall MF, Eckert RJ, Blakeway RD, Sterne TK, Hickerson EL, et al. Localized coral reef mortality event at East Flower Garden Bank, Gulf of Mexico. Bulletin of Marine Science. 2019; 95 (2):239–50.

15. Gruber N, Boyd PW, Frölicher TL, Vogt M. Biogeochemical extremes and compound events in the ocean. Nature. 2021; 600(7889):395–407. https://doi.org/10.1038/s41586-021-03981-7 PMID: 34912083

16. Chaudhary C, Richardson AJ, Schoeman DS, Costello MJ. Global warming is causing a more pronounced dip in marine species richness around the equator. PNAS. 2021; 118(15):1–6. https://doi.org/10.1073/pnas.2015094118 PMID: 33876750

17. Lucey N, Haskett E, Collin R. Multi-stressor extremes found on a tropical coral reef impair performance. Frontiers in Marine Science. 2020 Dec 9; 7.

18. Johnson MD, Scott JJ, Leray M, Lucey N, Bravo LMR, Wied WL, et al. Rapid ecosystem-scale consequences of acute deoxygenation on a Caribbean coral reef. Nature Communications. 2021 Dec 1; 12(1). https://doi.org/10.1038/s41467-021-24777-3 PMID: 34312399

19. Seemann J, Gonzalez CT, Carballo-Bolanos R, Berry K, Heiss GA, Struck U, et al. Assessing the ecological effects of human impacts on coral reefs in Bocas del Toro, Panama. Environmental Monitoring and Assessment. 2013;

20. Yeager DP, Ultsch GR. Physiological Regulation and Conformation: A BASIC Program for the Determination of Critical Points. Physiological Zoology. 1989 Jul 1; 62(4):888–907.

21. Hochachka PW, Somero GN. Biochemical adaptation: mechanism and process in physiological evolution. Oxford University Press; 2002.

22. Clark TD, Sandblom E, Jutfelt F. Aerobic scope measurements of fishes in an era of climate change: respirometry, relevance and recommendations. Journal of Experimental Biology. 2013; 216:2771–82. https://doi.org/10.1242/jeb.084251 PMID: 23842625

23. Masson-Delmotte, V., P. Zhai, A. Pirani, S.L. Connors, C. Péan, S. Berger, N. et al. IPCC, 2021: Climate Change 2021: The Physical Science Basis. Contribution of Working Group I to the Sixth Assessment Report of the Intergovernmental Panel on Climate Change (eds.)]. Cambridge University Press, Cambridge, United Kingdom and New York, NY, USA, 2021.

24. Deutsch C, Mcmanus J, Crusius J, Ito T, Baumgartner T. Centennial changes in North Pacific anoxia linked to tropical trade winds. Science. 2014; 665.

25. Takano Y, Ito T, Deutsch C. Projected centennial oxygen trends and their attribution to distinct ocean climate forcings. Global Biogeochemical Cycles. 2018; 32(9):1329–49.

26. Harianto J, Carey N, Byrne M. respR—An R package for the manipulation and analysis of respirometry data. Methods in Ecology and Evolution. 2019 Jun 1; 10(6):912–20.

27. Lutterschmidt WI, Hutchison VH. The critical thermal maximum: data to support the onset of spasms as the definitive end point. Canadian Journal of Zoology. 1997; 75:1553–60.

28. Vinagre C, Leal I, Mendonça V, Flores AAV. Effect of warming rate on the Critical Thermal Maxima of crabs, shrimp and fish. Journal of Thermal Biology. 2015; 47:19–25. https://doi.org/10.1016/j.jtherbio.2014.10.012 PMID: 25526650

29. Norin T, Clark TD. Measurement and relevance of maximum metabolic rate in fishes. Journal of Fish Biology. 2016; 88:122–51. https://doi.org/10.1111/jfb.12796 PMID: 26586591

30. Claireaux G, Chabot D. Responses by fishes to environmental hypoxia: integration through Fry' s concept of aerobic metabolic scope. Journal of Fish Biology. 2016; 88(1):232–51. https://doi.org/10.1111/jfb.12833 PMID: 26768976

31. Michael J. Crawley. The R Book. 2012.

32. Zuur AF, Ieno EN, Elphick CS. A protocol for data exploration to avoid common statistical problems. Statistical Methods In Evolution And Ecology. 2010;3–14.

33. R Core Team. R: A language and environment for statistical computing. Vienna, Austria; 2022.

34. Stohr S, O'Hara T, Thuy B. Global diversity of brittle stars (Echinodermata: Ophiuroidea). PLoS ONE. 2012; 7(3). https://doi.org/10.1371/journal.pone.0031940 PMID: 22396744